

A Move-and-Hold Pneumatic Actuator Enabled by Self-Softening Variable Stiffness Materials

Trevor L. Buckner, Edward L. White, Michelle C. Yuen, R. Adam Bilodeau, and Rebecca K. Kramer

Abstract—Materials exhibiting variable stiffness properties have great potential for use in the growing field of soft robotics. Soft structural materials allow a robot to fit into enclosed spaces, resist shock and vibration, or even reconfigure its geometry and adapt to various environments. Rigid structural materials on the other hand allow environmental interactions through application of force and load-bearing capabilities. Materials that can be selectively switched between these two extremes could greatly expand the functionality of a robot that requires the properties of both. In this paper, we introduce a conductive epoxy composite that is self-softening through Joule heating via direct application of electrical current. The polymer can then become load-bearing and rigid again after being formed into a new shape. We demonstrate the capabilities of this material by attaching a pneumatic actuator and showing that the resulting variable stiffness device can be softened from its initial rigid state, reshape itself using the pneumatic actuator, then become rigid again and hold this new position without additional power being supplied to the actuator.

I. INTRODUCTION

The relatively young field of soft robotics aims to introduce extended functionality to traditional mechanical and electronic systems by allowing highly flexible, extensible, or reconfigurable structures and components to take the place of traditional rigid, heavy, and bulky robotic parts. This allows the development of machines which are able to navigate unpredictable obstacles with adaptive geometries, fit inside confined spaces, and withstand violent forces or vibrations. These properties however, become disadvantageous when attempting to apply forces to other bodies or directly manipulate the environment in which the robot operates. Where traditional rigid robots can utilize their weight and stiff structure to impart forces on objects and support loads, soft robots instead tend to flow around the target object, collapse, or slip because they lack sufficient blocking force. In order to overcome this challenge, soft robots need a way to selectively adjust their stiffness to create rigid load paths on demand.

A brute-force solution to manipulation in soft systems is to create systems with large free displacements and low stiffness. This approach can generate the required blocked force, but at the cost of bulky actuators. Further, in the case of pneumatic actuators, the pressures required to achieve large blocked forces can create unworkably large stresses in non-contacting sections of the actuator. Finally, in many cases actuators must be left on to hold a blocked force, requiring the expenditure of energy to produce no work. An alternative approach is to use materials with variable stiffness to tune the mechanical

All authors are with the School of Mechanical Engineering Purdue University, West Lafayette, IN, USA {tbuckne, white335, yuenm, rbilodea, rebeccakramer}@purdue.edu



Fig. 1. Left: Softened variable stiffness pneumatic device inflated and supporting a 200g mass. Right: Supporting the same mass in a rigid material state with no power input. Weight is supported by a platform secured to the end of the finger.

response of a robotic system. This allows the robot to soften, actuate to the desired position, and then become rigid again without the need for continuous power input.

In this work, we introduce a robotic system comprised of an elastomer-based pneumatic actuator bonded to a novel, variable-stiffness, self-softening material. This system can be made to hold loads when in the rigid state, yet become flexible as desired to be reshaped into a new rigid configuration, shown in Figure 1. The material consists of a matrix of thermally-responsive shape memory polymer (SMP) with a conductive phase of expanded intercalated graphite (EIG). This composite material takes advantage of the low glass-transition temperature of the SMP thermoset, thus providing both a rigid and soft material state within a reasonable temperature range. The glass transition temperature can be reached through Joule heating by applying electric current directly to the conductive material. By combining the pneumatic actuator and variable stiffness material, we demonstrate that we are able to passively hold a deformed state under load and adjust component stiffness to achieve deformations at reasonable pneumatic pressures.

II. PREVIOUS WORK

There have been many research efforts exploring the actuation of soft robots. Materials have been reported that change shape in response to light, pH levels, heat, or other stimuli [1], such as shape memory alloys [2] and shape memory polymers [3]. Other solutions utilize fluidics [4] or electric motors coupled to cables [5]. However, these approaches rely on continuous input stimuli to maintain the modified shape or position, resulting in only intermittent functionality or large energy expenditures to maintain state under load. In addition to adjusting the shape of the robot,

there are a number of methods used to adjust the stiffness to structural parts [6]. These include pressure differentials [7], granular jamming [8], and changing shape to make use of geometric stiffening [9].

The method we have selected to achieve variable stiffness is the use of thermally responsive materials. Previous temperature-based approaches have demonstrated stiffness change through heating low-melting metallic alloys [10], [11], [12] or thermoplastics [13], [14], [15], [16] to achieve a state transition. Often methods involve an interface between two or more materials, with one acting as a heating element, and another as the variable-stiffness material. We have previously developed variable-stiffness fibers by encapsulating nickel titanium shape memory alloy wire in thermoplastic polymers which were softened by resistively heating the wire [17]. However, the approach of employing a discrete heating component inherently suffers from uneven thermal gradients, risk of component delamination, and complicated manufacturing steps due to the need for embedded elements and materials properly interfacing with each other.

There has been much research into adding conductive materials to various polymers to impart desirable electrical characteristics. These have been used to develop stretchable or printable electronics using conductive inks [18] or conductive 3D printer filament [19] and have been primarily accomplished with carbon black, graphene particles, carbon nanotubes, and metallic powders [20], [21], [22], [23]. However, these generally require high additive loading percentages to reach a sufficient level of conductivity, which in turn leads to processing difficulties [19]. Material properties are also affected by processing techniques; polymers require a low viscosity to effectively introduce additive particles, which often requires processing at high temperatures beyond the material melting point [24]. This causes difficulties especially when working with polymer blends of differing thermal characteristics [25]. Alternatively, our own experiments have shown that processing thermoplastics in a solvent lends itself to high porosity in the material as the solvent is evaporated, which in turn causes mechanical brittleness and poor electrical connectivity through the structure. The solution is often additional hot processing under compression to reach the final material shape and density [19]. Finally, previous attempts at using conductive polymers as variable stiffness materials have been successful, but require high voltages and exhibit limited stiffness on par with leather when in the rigid state, thus limiting the possibility for load-bearing applications [26].

Our novel composite material overcomes the issues mentioned above. We elected to use a thermally responsive epoxy as a base, which means a robotic device using this material in its structure would only need to expend energy during the softening and reshaping period; otherwise, the material remains rigid and load-bearing without expending energy. The composite is also intrinsically conductive yet retains mechanical robustness. This not only simplifies the device by reducing the number of distinct materials needed to function as a heater, but also eliminates the problems generated by interfacing with a discrete heating element. In



Fig. 2. Top: Variable stiffness sample in initial flat configuration. Bottom: Variable stiffness sample bent into a curve demonstrates passive holding of a deformed shape. The sample is approximately 10cm from end to end, not including the conductive fabric electrodes.

the rigid state, the stiffness of the material is comparable to acrylic, yet decreases by more than a full order of magnitude when softened. Finally, the material can be mixed at room temperature which facilitates processing and attaining homogeneous material properties.

III. MATERIALS AND MANUFACTURE

Samples of self-softening variable-stiffness material (VSM) were made by mixing together two liquid shape memory polymer (SMP) epoxy components with graphene particles, followed by curing for 12hr at 60°C in a silicone rubber mold. Sections of silver-coated nylon fabric (Adafruit) were embedded in either end to serve as electrical terminals. An SMP epoxy was selected partially for its ease of processing at room temperature while still in the liquid state. The SMP epoxy was created by combining an epoxy curing agent, Jeffamine D400 (Huntsman International, LLC), with a standard epoxy resin, EPON 828 (Momentive Performance Materials Inc.) at a ratio of 4:10 by weight [27].

The graphene particles were created by expanding intercalated graphite particles (Sigma-Aldrich) in an oven at 800°C for 5 minutes, and then sonicating in a 1wt% solution of cyclohexane for two hours at an amplitude of 36 μm (QSonica Q700 Ultrasonicator). This produces small graphene particles on the order of 50 nanometers in diameter. The solvent was then allowed to fully evaporate, leaving behind a dry aggregate of graphene in the form of a spongy solid. The graphene aggregate was then measured by weight and vigorously mixed into the uncured SMP epoxy by hand for several minutes until a uniform pasty consistency was reached. Samples were created at 5.0wt%, 7.5wt%, 10.0wt%, 12.5wt%, and 15.0wt% weight percent loading of graphene. When attempting to create mixtures of loadings higher than 15.0wt%, the resulting material became too dry to effectively incorporate all of the additive material; even after heavy mixing by hand, small pockets of loose graphene were left behind.

After mixing, the viscosity of the liquid epoxy increased, and the resulting composite had to be pressed into a silicone mold. In these experiments, a 100mm \times 25mm \times 2.8mm rectangular mold was used. A strip of conductive fabric was set into each end of the mold and coated over with composite

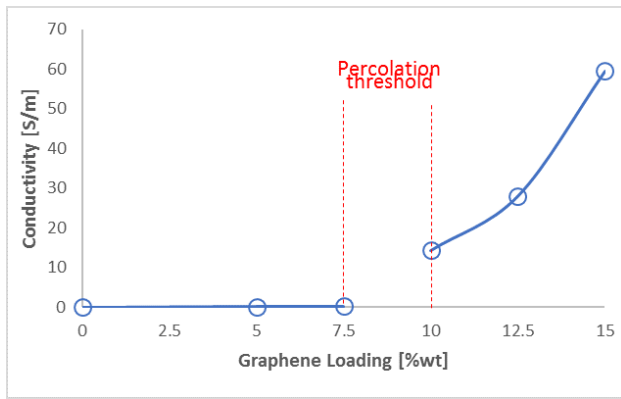


Fig. 3. Effect of graphene loading percentage on conductivity.

material until the mold was filled, and excess material was scraped from the top. The conductive SMP epoxy sample was then cured for 12hr at 60°C. After curing, samples were easily removed from the flexible mold. Completed samples in various rigid configurations are shown in Figure 2.

IV. CHARACTERIZATION

A. Electrical Properties

A preliminary study was conducted to determine the useful range of graphite loading to produce a heating element. Initial resistivity measurements were taken of samples at graphene loading percentages from 0.0wt% to 15.0wt%. It was found that samples at or below 7.5wt% loading had negligible conductivity. On the other hand, samples above 10.0wt% loading were found to have useful conductivity. As conductive additive content increases from 0.0wt%, the composite eventually reaches a critical loading percentage where the randomly-oriented filler particles begin to form continuous conducting paths. This is seen as a sudden increase in the conductivity of the material, and is known as the percolation threshold [28]. The percolation threshold can vary for each material depending on additive size, shape, and processing technique [25], [28]. This phenomenon becomes an important point as robotics increasingly makes use of new materials, particularly those that require modified electrical or thermal properties while largely retaining the physical characteristics of another material. From Figure 3, it can be seen that the percolation threshold for this VSM occurs somewhere between 7.5wt% and 10.0wt% graphene loading. This low threshold promotes improved mechanical properties of the material, as the brittleness imposed by high loading percentages is minimized. Further testing was only performed on the top three loading percentages (10.0wt%, 12.5wt%, and 15.0wt%) since samples of any loading lower than 10wt% essentially acted as insulators, thus making them unusable as heating elements.

A total of 15 additional samples (5 each of 10.0wt%, 12.5wt%, and 15.0wt% loading) were used for all further tests. The sets of 5 samples at each loading percentage were created from the same batch of material. By applying electrical current through each sample at varying levels of power, it was observed that the material exhibits a positive

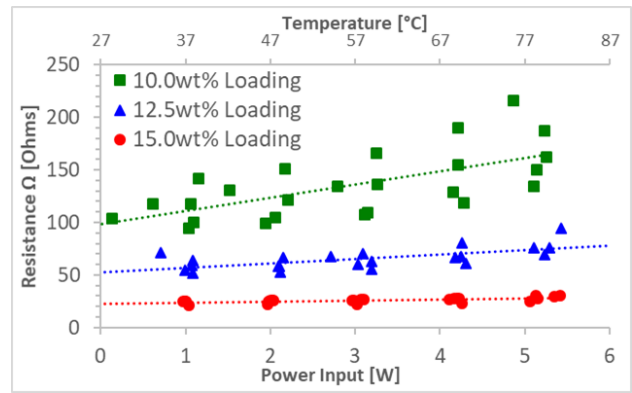


Fig. 4. Effect of increasing temperature on the material's electrical resistance. Note that lower loading percentages exhibit increased variability in measured resistance across all temperature levels. See Figure 6 for power-to-temperature conversion.

temperature coefficient of resistance, meaning the resistance increases as temperature rises. Resistance was measured at approximately 1 watt increments of applied power. At constant current, the rising resistance also caused the voltage to rise. Thus, the temperature and power were allowed to stabilize for three minutes before making the measurement. The resulting data reveals an approximately linear relationship between resistance and temperature, as shown in Figure 4. This is an interesting effect with potentially useful application, since a positive temperature coefficient material can be designed to predictably reach a maximum temperature for a given voltage; at some point any further increase in temperature would be met with greater electrical resistance, resulting in an equilibrium state.

Figure 4 also shows that the positive temperature coefficient is more pronounced at lower loadings of graphite. Also notable is the drastic influence the additive percentage has on the deviation in resistance, which may be an effect of the proximity to the percolation threshold. As the additive percentage approaches the percolation threshold, the probability of achieving a complete electrical bridge from end to end becomes less certain, thus making the material more susceptible to changes in resistance, and higher loading percentages would seem to grant more predictable electrical properties. A balance can be struck between consistent and desirable electrical properties (favoring higher loading percentages) and robust mechanical properties (favoring lower loading percentages). In this case, however, the 15wt% loading was found to exhibit no detrimental mechanical properties within the scope of the experiments performed, as detailed later in this work.

B. Thermal Properties

A differential scanning calorimetry (DSC) test was performed on the samples at 10.0wt% and 15.0wt% loading. This test is a thermo-analysis technique that measures the difference in heat flux between the sample and a reference, usually air, as a function of the temperature. This allows us to determine the temperature at physical state changes of the material. The samples were heated from -20°C to 200°C at 10°C/min, repeating the cycle 5 times per sample. Differences

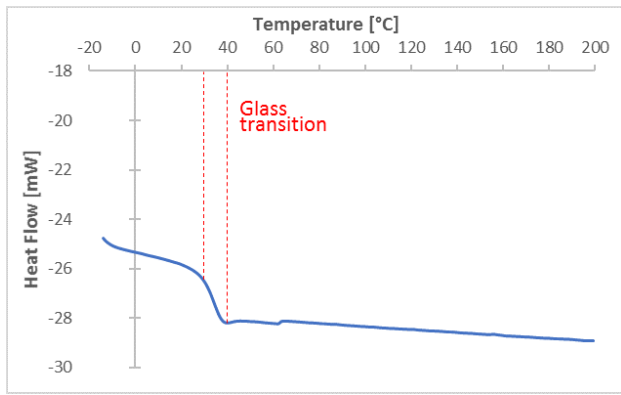


Fig. 5. Differential scanning calorimetry test of conductive SMP. Glass transition occurs between approximately 30°C and 40°C.

between the two loading percentages were negligible. The glass transition of the material was found to occur from 30°C to 40°C. The resulting plot is shown in Figure 5.

We also sought to correlate power input to temperature of the samples. Using a thermal camera, the maximum local steady-state temperatures at a range of power input levels (from 0 to 5W) was recorded on one sample from each loading percentage. During recording, samples were suspended on each end by a rubber stopper to minimize interference from thermal conduction. It was found that the final steady-state temperature formed a linear relationship with the input power. Results are shown in Figure 6.

C. Mechanical Properties

The 15 samples used in the earlier electrical properties tests (5 each of 10.0wt%, 12.5wt%, and 15.0wt% loading) were reused by testing at varying power input levels in a three-point bending test to determine the change in bending modulus as increasing power was applied. Samples were allowed three minutes to reach a stable temperature at each power level before running the bending test; samples tended to reach a steady state at approximately two and a half minutes. At constant current, we observed some voltage drift due to the positive temperature coefficient of resistance. To account for this, current was periodically adjusted such that the desired power level was attained at the final steady-state temperature.

Testing was conducted with an Instron 3345 fitted with a

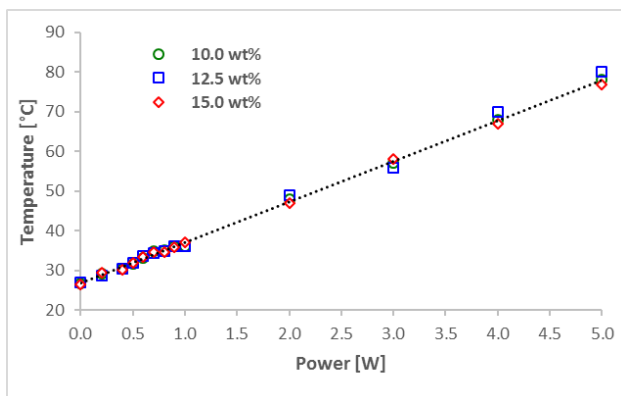


Fig. 6. Maximum temperature found with a thermal camera at various electrical power inputs, found to follow a linear trend.

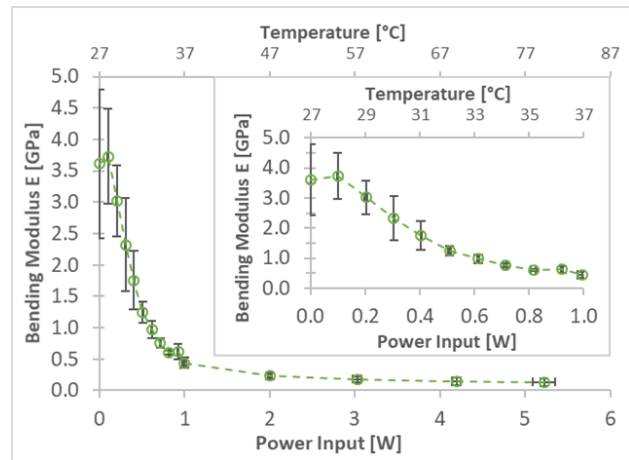


Fig. 7. Decreasing bending modulus with increasing power input at 15.0% graphite loading by weight. Temperature scale found in Figure 6 is included along the top axis.

TABLE I

AVERAGE BENDING MODULUS PROPERTIES AT THE STIFF (NO POWER) AND SOFT (5W POWER) STATES FOR DIFFERENT LOADING WEIGHTS

Loading	Rigid E [GPa]	Soft E [GPa]	Ratio
10.0wt%	1.88	0.0829	22.7
12.5wt%	2.30	0.0619	37.2
15.0wt%	3.61	0.132	27.7

50N load cell. The crosshead was moved at 10mm/min to a maximum displacement of 10mm; the supports were set 10cm apart, with the point of load application in the center. After bending, the sample was heated at 5W for 10 seconds to allow it to soften and return to the initial flat shape where it was held and allowed to cool by a fan for two minutes, at which point the sample was approximately at room temperature before testing at the next power level. The bending modulus was calculated from the force-displacement data collected at each power level. The resulting plot for this data on the 15% loading percentage is shown in Figure 7. Plots for the other two loading percentages follow the same trend, but are shifted downward slightly, suggesting that higher levels of graphite additive may have served to increase the overall stiffness of the material, as previous literature suggests [29]. The average bending modulus for the rigid and soft (5W) states of all three loading weights are listed in Table I.

The inset in Figure 7 shows a typical change in bending modulus in response to thermal stimulus for a thermoset polymer. Bending modulus is unchanged until around around 0.1W, then monotonically decreases until a plateau is reached at around 1W. This decrease in stiffness is a result of the glass transition, and appears to occur between 28°C and 38°C, which closely matches with our results from DSC testing. Sources of the small 2°C discrepancy between the two could be due to temperature gradients within the material samples, as well as a temperature lag between the material sample and the recorded DSC temperatures. In each test however, the entire glass transition occurs over a range of approximately 10°C. Increasing the power does cause the material to reach its rubbery state more quickly (1 minute at 1W, but within 10 seconds at 5W), but further changes in stiffness after the

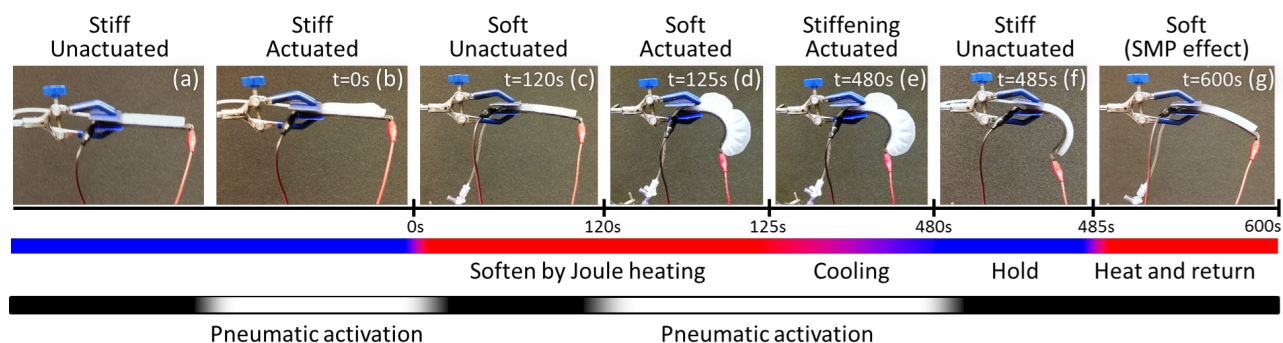


Fig. 8. Demonstration of self-softening variable stiffness material in conjunction with a pneumatic actuator. (a),(b) The pneumatic actuator is unable to bend the material when in the rigid state. (c) VSM is heated and softened. (d) Soft VSM can be bent by the actuator. (e) Pneumatic actuator holds position while the VSM cools. (f) Pressure is released and VSM retains actuated position. (g) Further heating demonstrates the shape memory effect of the material and elasticity of the pneumatic which pulls the device back to near the initial position.

glass transition are greatly reduced, although not negligible; the stiffness of a sample heated with 5W is approximately one-fourth the stiffness when heated with 1W. Based on these tests, an average change in stiffness of more than an order of magnitude can be reached using only 2 watts. This significant change is comparable to a transition from acrylic to a polymer foam. In the rigid state, the material can be used to support significant loads with minimal deflection; in the soft state, the material can be reshaped with small forces. For example, after attaching a sample of this material to our pneumatic actuator, we found that a pressure of 15kPa was required to bend it at 1W power. However, when fully cooled and rigid, the actuator required 117kPa to bend it.

It is also interesting to note that the uncertainty in the modulus increases drastically at lower power levels. This may be partially due to differences in the amount of polymer chain conformation, polymer crosslinking, or manufacturing defects across samples which become more evident near the crystalline phase of the material, but begin to diminish as the epoxy approaches a rubbery state and polymer chains are able to shift more freely. Due to the very low glass transition temperature, other sources of discrepancy could be the effects of fluctuating ambient temperature at low power levels. A difference of only a couple degrees can create a large change in stiffness. This can be favorable due to the relatively low operating temperatures and narrow temperature ranges required to enact stiffness switching. However, this also introduces complexity and uncertainty if attempting to tune device stiffness to a specific value, especially within the glass transition range.

V. APPLICATIONS

We demonstrate the effectiveness of this material in conjunction with a silicone pneumatic actuator, shown in Figure 8. The VSM is initially in the rigid glassy state, and the pneumatic actuator inflated by hand to 15kPa is unable to bend it at all. However, as 3W of electric power is applied, the material begins to soften. After one minute, the actuator can then easily bend the material to a new position, where it is held for 6min while the VSM cools. After cooling, the VSM has become rigid once again and holds the new shape. An interesting effect of the SMP is the shape memory

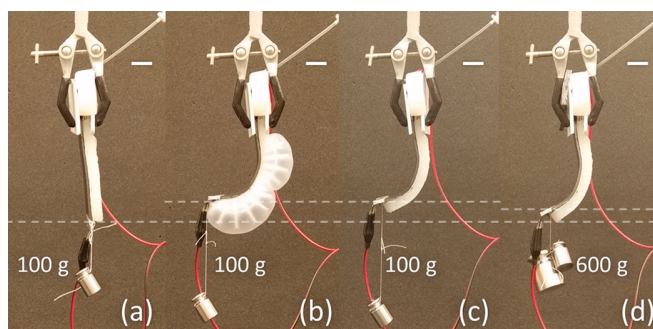


Fig. 9. Pneumatic actuator lifting weights. Scale bars are 2cm. (a) VSM softened. (b) Actuator is able to lift a 100g weight. (c). VSM stiffened after cooling for 6 minutes, still holding the 100g weight. (d) Added a 500g weight to the load. The VSM sags very slightly but still holds the weight.

effect which, in combination with the elastic properties of the pneumatic actuator, is able to return the device nearly to its original position. A second actuator on the opposite side could easily provide the needed force to bend the device in the other direction or return it to the original flat configuration.

In another demonstration (Figure 9), we show that the pneumatic actuator can be used to lift masses with the VSM in the soft state, and can then hold the masses in position using only the stiffened VSM. At 15kPa, the pneumatic actuator is only able to lift 100g to a height of approximately 2cm. With this mass held by the actuator, the VSM is allowed to cool for 6 minutes to the rigid state. Interestingly, after releasing the pneumatic pressure, the VSM is not only able to keep the 100g mass suspended without detectable sagging, but is also able to support an added mass, totaling 600g before substantially deforming (a drop of about 0.6cm is visible in the figure). In the soft state, the VSM is not contributing structurally to the support of the mass; the inflated pneumatic is stiffer than the softened VSM and is solely responsible for the lifting capability. In the stiff state, the opposite is true; the VSM is much stiffer than the inflated pneumatic, allowing it to support much more weight than the actuator on its own.

VI. CONCLUSION AND FUTURE WORK

We have developed a robotic device by combining an elastomer-based pneumatic actuator with a novel material which exhibits variable-stiffness properties and is activated

through simple application of low power electricity. This material can be processed with a straightforward manufacturing process and molded into any desired shape. The robotic system is able provide a repeatable order-of-magnitude change in stiffness allowing move-and-hold operations, supporting significant mass with minimal deformation and without continuous energy expenditure. This technology has potential for use in the growing field of soft robotics, enabling increased functionality and adaptability for future robotic designs by enhancing the load-bearing capability, actuator effectiveness, and energy-efficiency of soft machines.

Since temperature-dependent systems intrinsically suffer from long cooling times, future work will consider both material and geometry in an effort to shorten the softening and stiffening cycle length. Additional follow-up will investigate integration of the VSM with other forms of actuation, including different pneumatic designs, shape-memory alloys, and cable-driven mechanisms. The highly-viscous nature of the uncured VSM makes it an ideal candidate for molding or extruding into arbitrary shapes, embedding into fabric substrates, and 3D printing. Using these techniques, new geometric designs will be tested to allow for movement in three dimensions and elongation in tension.

ACKNOWLEDGMENT

This work was primarily supported by the Air Force Office of Scientific Research under award number FA9550-16-1-0267. ELW and MCY are supported under the National Science Foundation Graduate Research Fellowship program (DGE-1333468). RAB is supported by an Early Career Faculty grant from NASA's Space Technology Research Grants program (NNX14AO52G).

REFERENCES

- [1] H. Meng and G. Li, "A review of stimuli-responsive shape memory polymer composites," vol. 54, no. 9, pp. 2199–2221. [Online]. Available: <http://www.sciencedirect.com/science/article/pii/S0032386113001444>
- [2] M. Yuen, A. Cherian, J. C. Case, J. Seipel, and R. K. Kramer, "Conformable actuation and sensing with robotic fabric," in *2014 IEEE/RSJ International Conference on Intelligent Robots and Systems*, pp. 580–586.
- [3] A. Lendlein and R. Langer, "Biodegradable, elastic shape-memory polymers for potential biomedical applications," vol. 296, no. 5573, pp. 1673–1676. [Online]. Available: <http://science.sciencemag.org/content/296/5573/1673>
- [4] R. F. Shepherd, F. Ilievski, W. Choi, S. A. Morin, A. A. Stokes, A. D. Mazzeo, X. Chen, M. Wang, and G. M. Whitesides, "Multigait soft robot," vol. 108, no. 51, pp. 20400–20403. [Online]. Available: <http://www.pnas.org/content/108/51/20400>
- [5] M. Calisti, M. Giorelli, G. Levy, B. Mazzolai, B. Hochner, C. Laschi, and P. Dario, "An octopus-bioinspired solution to movement and manipulation for soft robots," vol. 6.
- [6] M. Manti, V. Cacucciolo, and M. Cianchetti, "Stiffening in soft robotics: A review of the state of the art," vol. 23, no. 3, pp. 93–106.
- [7] Ying Shan, M. Philen, A. Lotfi, Suyi Li, C. E. Bakis, C. D. Rahn, and K. Wang, "Variable stiffness structures utilizing fluidic flexible matrix composites," vol. 20, no. 4, pp. 443–456. [Online]. Available: <http://journals.sagepub.com/doi/abs/10.1177/1045389X08095270>
- [8] A. Jiang, G. Xynogalas, P. Dasgupta, K. Althoefer, and T. Nanayakkara, "Design of a variable stiffness flexible manipulator with composite granular jamming and membrane coupling," in *2012 IEEE/RSJ International Conference on Intelligent Robots and Systems*, pp. 2922–2927.
- [9] S.-H. Song, M.-S. Kim, H. Rodrigue, J.-Y. Lee, J.-E. Shim, M.-C. Kim, W.-S. Chu, and S.-H. Ahn, "Turtle mimetic soft robot with two swimming gaits," vol. 11, no. 3, p. 036010.
- [10] A. Tonazzini, S. Mintchev, B. Schubert, B. Mazzolai, J. Shintake, and D. Floreano, "Variable stiffness fiber with self-healing capability," vol. 28, no. 46, pp. 10142–10148. [Online]. Available: <http://onlinelibrary.wiley.com/doi/10.1002/adma.201602580/abstract>
- [11] B. E. Schubert and D. Floreano, "Variable stiffness material based on rigid low-melting-point-alloy microstructures embedded in soft poly(dimethylsiloxane) (PDMS)," vol. 3, no. 46, pp. 24671–24679. [Online]. Available: <http://pubs.rsc.org/en/Content/ArticleLanding/2013/RA/c3ra44412k>
- [12] J. Shintake, B. Schubert, S. Rosset, H. Shea, and D. Floreano, "Variable stiffness actuator for soft robotics using dielectric elastomer and low-melting-point alloy," in *2015 IEEE/RSJ International Conference on Intelligent Robots and Systems (IROS)*, pp. 1097–1102.
- [13] T. P. Chenal, J. C. Case, J. Paik, and R. K. Kramer, "Variable stiffness fabrics with embedded shape memory materials for wearable applications." [Online]. Available: <https://infoscience.epfl.ch/record/206392>
- [14] N. G. Cheng, A. Gopinath, L. Wang, K. Iagnemma, and A. E. Hosoi, "Thermally tunable, self-healing composites for soft robotic applications," vol. 299, no. 11, pp. 1279–1284. [Online]. Available: <http://onlinelibrary.wiley.com/doi/10.1002/mame.201400017/abstract>
- [15] J. R. Capadona, K. Shanmuganathan, D. J. Tyler, S. J. Rowan, and C. Weder, "Stimuli-responsive polymer nanocomposites inspired by the sea cucumber dermis," vol. 319, no. 5868, pp. 1370–1374. [Online]. Available: <http://science.sciencemag.org/content/319/5868/1370>
- [16] M. A. McEvoy and N. Correll, "Thermoplastic variable stiffness composites with embedded, networked sensing, actuation, and control," vol. 49, no. 15, pp. 1799–1808. [Online]. Available: <http://journals.sagepub.com/doi/abs/10.1177/0021998314525982>
- [17] M. C. Yuen, R. A. Bilodeau, and R. K. Kramer, "Active variable stiffness fibers for multifunctional robotic fabrics," vol. 1, no. 2, pp. 708–715.
- [18] L. Huang, Y. Huang, J. Liang, X. Wan, and Y. Chen, "Graphene-based conducting inks for direct inkjet printing of flexible conductive patterns and their applications in electric circuits and chemical sensors," vol. 4, no. 7, pp. 675–684. [Online]. Available: <https://link.springer.com/article/10.1007/s12274-011-0123-z>
- [19] S. J. Leigh, R. J. Bradley, C. P. Purssell, D. R. Billson, and D. A. Hutchins, "A simple, low-cost conductive composite material for 3d printing of electronic sensors," vol. 7, no. 11, p. e49365. [Online]. Available: <https://www.ncbi.nlm.nih.gov/pmc/articles/PMC3504018/>
- [20] L. Lu, F. Zhang, J. Xia, Z. Wang, and Y. Yuan, *Conductive Carbon Black-Graphene Composite for Sensitive Sensing of Ruin*.
- [21] J. Li, P. C. Ma, W. S. Chow, C. K. To, B. Z. Tang, and J.-K. Kim, "Correlations between percolation threshold, dispersion state, and aspect ratio of carbon nanotubes," vol. 17, no. 16, pp. 3207–3215. [Online]. Available: <http://onlinelibrary.wiley.com/doi/10.1002/adfm.200700065/abstract>
- [22] P. C. Ma, B. Z. Tang, and J.-K. Kim, "Effect of CNT decoration with silver nanoparticles on electrical conductivity of CNT-polymer composites," vol. 46, no. 11, pp. 1497–1505. [Online]. Available: <http://www.sciencedirect.com/science/article/pii/S0008622308003266>
- [23] Y. Lim, C. Lee, H. Choi, and J. Bae, "Fabrication of electrically conductive substrates using copper nanoparticles-deposited carbon black," p. 0021998316674266. [Online]. Available: <http://journals.sagepub.com/doi/abs/10.1177/0021998316674266>
- [24] G. Yu, M. Q. Zhang, H. M. Zeng, Y. H. Hou, and H. B. Zhang, "Conductive polymer blends filled with carbon black: Positive temperature coefficient behavior," vol. 39, no. 9, pp. 1678–1688. [Online]. Available: <http://onlinelibrary.wiley.com/doi/10.1002/pen.11562/abstract>
- [25] M. Sumita, K. Sakata, S. Asai, K. Miyasaka, and H. Nakagawa, "Dispersion of fillers and the electrical conductivity of polymer blends filled with carbon black," vol. 25, no. 2, pp. 265–271. [Online]. Available: <http://link.springer.com/article/10.1007/BF00310802>
- [26] W. Shan, S. Diller, A. Tutcuoglu, and C. Majidi, "Rigidity-tuning conductive elastomer," vol. 24, no. 6, p. 065001. [Online]. Available: <http://stacks.iop.org/0964-1726/24/i=6/a=065001>
- [27] I. A. Rousseau and T. Xie, "Shape memory epoxy: Composition, structure, properties and shape memory performances," vol. 20, no. 17, pp. 3431–3441. [Online]. Available: <http://pubs.rsc.org/en/content/articlelanding/2010/jm/b923394f>
- [28] J. Li and J.-K. Kim, "Percolation threshold of conducting polymer composites containing 3d randomly distributed graphite nanoplatelets," vol. 67, no. 10, pp. 2114–2120. [Online]. Available: <http://www.sciencedirect.com/science/article/pii/S0266353806004386>
- [29] A. Plymill, R. Minneci, D. A. Greeley, and J. Gritton, "Graphene and carbon nanotube PLA composite feedstock development for fused deposition modeling."